Eur Respir J 2005; 25: 534–544
DOI: 10.1183/09031936.05.00105804

Prone position reduces lung stress and strain in severe acute respiratory distress syndrome

S.D. Mentzelopoulos*, C. Roussos# and S.G. Zakynthinos#

ABSTRACT: The present authors hypothesised that in severe acute respiratory distress syndrome (ARDS), pronation may reduce ventilator-induced overall stress (*i.e.* transpulmonary pressure (P_L)) and strain of lung parenchyma (*i.e.* tidal volume (V_T)/end-expiratory lung volume (EELV) ratio), which constitute major ventilator-induced lung injury determinants. The authors sought to determine whether potential pronation benefits are maintained in post-prone semirecumbent (SR_{PP}) posture under pressure-volume curve-dependent optimisation of positive end-expiratory pressure (PEEP).

A total of 10 anesthetised/paralysed, mechanically ventilated ($V_T = 9.0 \pm 0.9$ mL·kg^{-1} predicted body weight; flow $= 0.91 \pm 0.04$ L·s^{-1}; PEEP $= 9.4 \pm 1.3$ cmH_2O) patients with early/severe ARDS were studied in pre-prone semirecumbent (SR_{BAS}), prone, and SR_{PP} positions. Partitioned respiratory mechanics were determined during iso-flow (0.91 L·s^{-1}) experiments (V_T varied within 0.2–1.0 L), along with haemodynamics, gas exchange, and EELV.

Compared with SR_{BAS}, pronation/SR_{PP} resulted in reduced peak/plateau P_L at V_Ts ≥ 0.6 L; static lung elastance and additional lung resistance decreased and chest wall elastance (in prone position) increased; EELV increased (23–33%); V_T/EELV decreased (27–33%); arterial oxygen tension/inspiratory oxygen fraction and arterial carbon dioxide tension improved (21–43/10–14%, respectively), and shunt fraction/physiological dead space decreased (21–50/20–47%, respectively).

In early/severe acute respiratory distress syndrome, pronation under positive end-expiratory pressure optimisation may reduce ventilator-induced lung injury risk. Pronation benefits may be maintained in post-prone semirecumbent position.

KEYWORDS: Acute respiratory distress syndrome, gas exchange, lung recruitment, mechanical ventilation, mechanics of the respiratory system, prone position

AFFILIATIONS
*University of Athens Medical School, Dept of Intensive Care Medicine, Attikon University Hospital, and
#University of Athens Medical School, Dept of Intensive Care Medicine, Evaggelismos General Hospital, Athens, Greece.

CORRESPONDENCE
S.D. Mentzelopoulos
12 Ioustinianou Street
GR-11473
Athens
Greece
Fax: 30 2103218493
E-mail: sdm@hol.gr

Received:
September 09 2004
Accepted after revision:
November 19 2004

SUPPORT STATEMENT
The present work was funded solely by the Dept of Intensive Care Medicine, University of Athens Medical School, Evaggelismos General Hospital, Athens, Greece.

In mechanically ventilated patients, lung stress and strain are major determinants of ventilator-induced lung injury (VILI) [1–5]. Alveolar stress (*i.e.* transmural pressure) is the ratio of alveolar wall tension to thickness. Thus, plateau/peak transpulmonary pressure (P_L) reflects overall lung parenchymal stress [2, 3]. Strain is distending force-induced lung parenchyma deformation, and corresponds to the tidal volume (V_T)/end-expiratory lung volume (EELV) ratio [3].

Acute respiratory distress syndrome (ARDS) patients are VILI susceptible, due to disorder-induced lung regional collapse/consolidation, which severely constrains normally aerated lung parenchyma [6–8]. VILI prevention comprises low V_T use, positive end-expiratory pressure (PEEP), and prone positioning [3]. Low V_T ventilation (6 mL·kg^{-1}) may not be advantageous relative to ''standard'' V_T ventilation (8–9 mL·kg^{-1}) [9]. PEEP may cause circulatory depression [10], increase pulmonary oedema [11, 12], and contribute to VILI by inducing lung regional overdistension [12, 13]. In severe ARDS with diffuse and bilateral aeration loss [8, 13, 14], PEEP-induced overinflation risk is reduced, even at high PEEP (17 cmH_2O) [15]. However, lung overdistension (excessive pressure applied to acutely-injured parenchyma) can occur without concomitant overinflation [14]; consequently, the rationale for optimal PEEP level selection (PEEP optimising arterial oxygenation and minimising oxygen toxicity/VILI risks) still holds. Prone positioning may attenuate VILI [15–17]. Prone position causes more homogenous lung inflation

European Respiratory Journal
Print ISSN 0903-1936
Online ISSN 1399-3003

and eliminates lung compression by the heart and abdominal contents, thus limiting atelectasis [14, 18, 19]. Semirecumbent positioning may also attenuate cardiac/abdominal lung compression relative to a supine position [14]. Consequently, in severe ARDS, the elucidation of the effects of PEEP/body positioning optimisation [14] with respect to major VILI determinants might be of considerable clinical importance.

The present authors tested the hypothesis that following PEEP optimisation, prone positioning may reduce P_L and V_T/EELV relative to pre-prone semirecumbent (SR_{BAS}) in patients with early/severe ARDS. The current authors also sought to determine whether the potential pronation benefits are maintained in the post-prone semirecumbent (SR_{PP}) posture. Total respiratory system (RS), chest wall and lung mechanics, and haemodynamics/gas exchange were also determined and compared among the aforementioned body postures.

MATERIAL AND METHODS

Patients

Institutional Review Board (Evaggelismos General Hospital, Scientific Committee, Athens, Greece) approval and informed/written next-of-kin consent were obtained. A total of 10 consecutive patients with early (disorder diagnosis established within the preceding 72 h) and severe ARDS (table 1) [20] were enrolled between July 14, 2003 and July 12, 2004. ARDS was defined as acute onset, arterial oxygen tension (P_{a,O_2})/inspiratory oxygen fraction (F_{I,O_2}) <200 mmHg (regardless of PEEP level), bilateral infiltrates on frontal chest radiograph, and wedge pressure <18 mmHg [21]. Inclusion criteria with respect to ARDS severity were $P_{a,O_2}/F_{i,O_2} \leqslant 100$ mmHg, and a ''white lungs'' feature (hyperattenuation areas equally disseminated within upper and lower lung lobes) [20] on frontal chest radiograph. Radiographs were independently evaluated by two independent radiologists. Exclusion criteria included age <18 yrs, pregnancy, intracranial hypertension, burns >30% of body surface area, spine fractures, smoking and/or chronic respiratory disease, chronic liver disease (Child-Pugh class C) [22], neuromuscular disease impairing spontaneous breathing, sickle cell disease, and body mass index >27.5 $kg \cdot m^{-2}$.

During the 6-h duration study-period, patient care was provided by an independent physician. New/additional administration of *i.v.* fluid boluses, inotropes, antipyretics, antiarrhythmic treatment, or diuretics led to patient exclusion

TABLE 1 Patient characteristics prior to inclusion to the study

Patient No.	Age yrs	Sex	BMI $kg \cdot m^{-2}$	SAPS II score#	Murray Score¶	$P_{a,O_2}/F_{I,O_2}$ mmHg¶	P_{a,CO_2} mmHg¶	F_{I,O_2}¶	PEEPe cmH_2O¶	V_T L/V_T $mL \cdot kg^{-1}$ PBW¶	$P_{2,aw}$ cmH_2O¶	Respiratory disease	Outcome
1	50	M	22.4	51	3.25	96.3	48.2	0.7	11	0.49/6.9	25.3	Staphylococcus Pneumonia+	S
2	40	M	21.7	52	3.50	94.4	49.2	0.7	12	0.48/7.1	26.6	Legionella Pneumonia§	S
3	43	F	21.3	59	3.75	91.1	51.1	0.8	13	0.51/9.1	35.0	Streptococcus Pneumonia+	D
4	33	M	22.2	53	3.50	88.9	52.3	0.8	13	0.49/7.1	29.3	Legionella Pneumonia§	S
5	26	M	23.1	54	4.00	79.0	52.5	0.8	14	0.5/7.0	33.2	Staphylococcus Pneumonia+	D
6	52	F	20.7	61	3.75	83.3	48.8	0.8	14	0.5/8.5	32.9	Klebsiella Pneumonia+	S
7	47	M	23.5	50	3.25	93.8	52.4	0.7	11	0.5/7.1	27.7	Streptococcus Pneumonia+	S
8	37	M	21.7	82	4.00	76.0	50.9	0.9	16	0.45/6.2	39.5	Staphylococcus Pneumonia+	D
9	44	M	21.4	79	4.00	79.1	50.3	0.9	16	0.46/6.3	39.8	Staphylococcus Pneumonia+	D
10	34	F	22.6	62	3.25	93.3	49.3	0.8	14	0.49/8.4	29.1	Streptococcus Pneumonia+	S

Patient No. refers to the order of enrolment to the study. Patients were mechanically ventilated at volume assist-control mode; inspiratory flow ranged within 0.6–0.9 $L \cdot s^{-1}$; respiratory rate (range 19–28·min^{-1}) was adjusted to maintain an arterial pH of $\geqslant$7.30. For males, predicted body weight was calculated as =50+(Height (cm)–152.4) × 0.91; for females, 50 was replaced by 45.5. Patients weaned from mechanical ventilation and discharged from the intensive care unit (ICU) were considered as survivors. BMI: body mass index; SAPS II: simplified acute physiology score II; P_{a,O_2}: arterial oxygen tension; F_{I,O_2}: inspiratory oxygen fraction; P_{a,CO_2}: carbon dioxide arterial tension; PEEPe: externally applied positive end-expiratory pressure; V_T: tidal volume; PBW: predicted body weight; $P_{2,aw}$: plateau tracheal pressure; M: male; S: survival; F: female; D: death (in the ICU). #: on ICU admission; ¶: variables recorded just prior to study enrolment, whilst there was no patient-ventilator asynchrony in any case; +: microorganism isolated in tracheobronchial aspirates (positive cut-off value=10^5 colony forming units·mL^{-1}); §: diagnosis established by PCR for Legionella and detection of Legionella antigen in urine.

[23]. Electrocardiographic lead II, peripheral intra-arterial and pulmonary artery (continuous cardiac output/S_{v,O_2} catheter; Baxter, Deerfield, IL, USA) pressures, urinary bladder temperature, and peripheral oxygen saturation (S_{a,O_2}) were monitored continuously [23].

Mechanical ventilation

Prior to study enrolment, patients were sedated (propofol/fentanyl infused at 3.5–4.0 mg·kg^{-1}·h^{-1}/1.5–2.0 μg·kg^{-1}·h^{-1}, respectively), orotracheally intubated and mechanically ventilated (Siemens 300C ventilator; Siemens AG, Berlin, Germany) in a ''near-supine'' position (20–30° inclination relative to horizontal). Intermittent neuromusculuar blockade was employed according to recent recommendations [24]. PEEP (13.4±1.8 cm H_2O), F_{I,O_2} (0.79±0.07), and breathing rate·min^{-1} (range 19–28) were set according to the ARDS Network protocol [25] (table 1). V_T (0.49±0.02 L=7.4±0.9 mL·kg^{-1} predicted body weight (PBW)) was adjusted so that plateau tracheal pressure ($P_{2,aw}$) was <35 cmH_2O, or kept within 6.0–6.5 mL·kg^{-1} PBW if $P_{2,aw}$ exceeded 35 cmH_2O (table 1). S_{a,O_2} achieved was 93.4±1.1%. Following study enrolment, anaesthesia and neuromuscular blockade were induced/maintained with additional propofol/fentanyl (induction bolus=0.5 mg·kg^{-1}/50 μg and maintenance infusion=3.5–4.0 mg·kg^{-1}·h^{-1}/1.5–2.0 μg·kg^{-1}·h^{-1}, respectively) and cisatracurium (intermittent administration targeted to full train-of-four inhibition throughout the study-period [23]), respectively, and body posture was changed to ''steep'' semirecumbent (60° inclination, SR_{BAS}). Prior to cisatracurium administration, oesophageal and gastric balloons were inserted and their correct placement was verified as previously described [26–28]. Study-period baseline ventilator settings (volume-controlled mode) were: F_{I,O_2}=0.79±0.07 (as above); V_T=0.6±0.03 L (9.0±0.9 mL·kg^{-1} PBW); inspiratory flow (V')=0.91±0.04 L·s^{-1}; breathing rate·min^{-1}=16–25 (adjusted to maintain an arterial pH>7.30) [24]; plateau pressure time=0 s; and PEEP=9.4±1.3 cm H_2O. PEEP was set at 2.0 cmH_2O above the lower inflection points of the pressure-volume curves, which were constructed as previously reported [20]. PEEP adjustment should not cause a $P_{a,O_2}/F_{I,O_2}$ decrease of >5 mmHg. Employed PEEP/V_T should not result in a plateau P_L ($P_{2,L}$) >30 cmH_2O. $SR_{PP}S_{a,O_2}$ was 92.0±1.0%.

Protocol and measurements

Investigational interventions were separated by 15 min of baseline ventilation for the re-establishment of baseline conditions [29]. Patients were sequentially studied in the SR_{BAS}, prone (0° inclination), and SR_{PP} (60° inclination) postures (2-h study duration for each posture). Patient turning was performed as previously described [23]. Following pronation, abdominal movement restriction was minimised as in previous studies [23, 30]. Any pronation-induced hypoxaemia (S_{a,O_2} ⩽90%) would result in protocol termination, and body posture change with ventilatory parameter adjustment as necessary. The reliability of oesophageal pressure (P_{oes}) measurements was tested as before (fig. 1) [23].

The P_{oes} tracing in figure 1d is the average of the tracings of the four sigh test breaths administered to the patient; all other tracings originate from the first of the four test sighs. On individual test breath P_{oes} tracings (figure 1e), the maximal amplitude of each cardiac oscillation was measured as the difference between oscillation peak pressure (P_{peak}) and the immediately preceding inspiratory plateau pressure ($P_{i,plateau}$). For each cardiac oscillation, P_{oes} rise rate was determined as the time needed for P_{oes} to rise from $P_{i,plateau}$ to P_{peak} during that particular oscillation. For each P_{oes} tracing, the mean maximal amplitudes of all cardiac oscillations, and mean P_{oes} rise rates during these oscillations were analysed; for each set

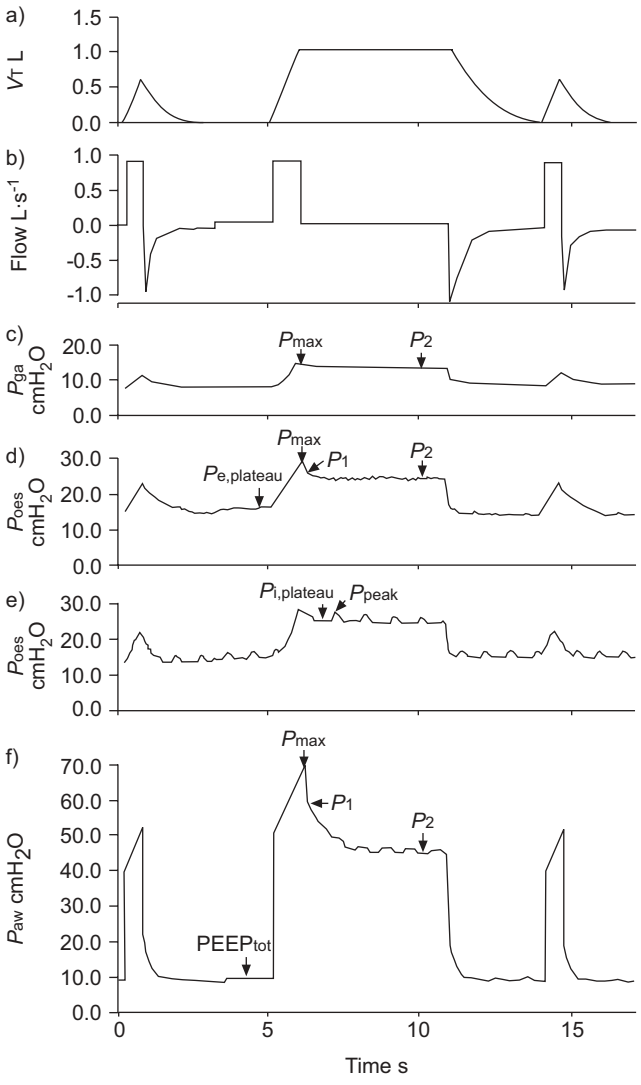

FIGURE 1. Assessment of respiratory mechanics. Presented variable data originate from a representative study participant. a) Tidal volume (V_T), b) flow, and c) gastric (P_{ga}), d and e) oesophageal (P_{oes}) and f) tracheal pressure (P_{aw}) data printout, showing two baseline ventilation mechanical breaths (V_T=0.6 L; inspiratory flow=0.91 L·s^{-1}) separated by a ''sigh'' test breath (V_T=1.0 L; inspiratory flow=0.91 L·s^{-1}). P_{max}: peak inspiratory pressure; P_2: plateau inspiratory pressure; $P_{e,plateau}$: end-expiratory occlusion plateau pressure of P_{oes}; P_1: pressure immediately after end-inspiratory airway occlusion; $P_{i,plateau}$: inspiratory plateau pressure; P_{peak}: oscillation peak pressure; $PEEP_{tot}$: total positive end-expiratory pressure. P_{aw} values were referred to atmospheric pressure. P_{ga} and averaged P_{oes} values were referred to respective values at respiratory system relaxation volume. $P_{e,plateau}$ was used for determination of $PEEP_{tot}$ of the chest wall.

of test breaths, the aforementioned variables were averaged and compared among study postures.

Respiratory mechanics

Inspiratory flow (V'), V_T, and tracheal (P_{aw}), P_{oes}, and gastric (P_{ga}) pressures were measured with a Hans-Rudolph pneumotachograph (pneumotachometer; Hans Rudolph Inc., Kansas City, MT, USA) and Validyne pressure-transducers (Validyne, Nortridge, CA, USA) [23]. Following analogue-to-digital conversion, variable data were stored on an IBM-type computer for later analysis with Anadat software (RHT-InfoData, Montreal, QC, Canada) [23]. During data sampling, variable tracings were displayed on a dedicated monitor and recorded (Gould ES 1000 electrostatic recorder; Gould Electronics Inc., Eastlake, OH, USA). Breathing circuit modifications included humidifier-removal and low compliance tubing [23]. Care was taken to avoid gas leaks. Equipment dead space (endotracheal tube (ETT) not included) was 90 mL.

Respiratory mechanics were assessed with constant V' rapid airway occlusion. Within 30–60 min after study-posture assumption, sets of four test breaths were administered with a constant, square-wave V' (0.91 $L \cdot s^{-1}$). V_T was sequentially varied from 0.6 (baseline) to 0.2, 0.4, 0.6, 0.8, and 1.0 (''sigh'') L. During sighs, the maximum allowable $P_{2,L}$ was 45 cm H_2O. Test breaths were separated by 1-min baseline ventilation periods (fig. 1).

Test breaths were preceded by 2-s duration end-expiratory occlusions, enabling determination of RS, chest wall, and abdominal chest wall-component total PEEP ($PEEP_{tot}$) (fig. 1); the latter was always ~0. For P_{oes}, end-expiratory occlusion-plateaus were obtained by ensemble averaging [31] of P_{oes} tracings of each test breath-set (fig. 1). Expiratory occlusions were followed by 4–6-s duration end-inspiratory occlusions, enabling determination of maximal pressure (P_{max}), and pressure immediately after initiation of end-inspiratory occlusion (P_1), and plateau pressure (P_2) on computer-stored P_{aw} tracings, and of P_{max} and P_2 on computer-stored P_{ga} tracings (fig. 1). For P_{oes}, P_{max}/P_1 and P_2, values were determined after ensemble tracing-averaging of each set of test breaths [31] (fig. 1). P_{aw} values were referred to atmospheric pressure, and P_{oes}/P_{ga} values were referred to their values at respiratory system relaxation volume (V_r); the latter values were determined during the below-described measurements of the change (Δ) in functional residual capacity (FRC). For each set of test breaths, P_L was determined as the difference between the average P_{aw} value and the averaged P_{oes}. Total RS, chest wall, and lung inspiratory mechanical properties were computed by standard formulas (see Appendix 1).

Haemodynamics and gas exchange

In each posture, intravascular pressure transducers (Abbott, Sligo, Ireland) were set to zero at right-atrial level. Within 75–90 min after posture assumption, end-expiratory central venous and pulmonary artery wedge pressures were determined consecutively three times during respective 10-s duration ETT disconnections from the breathing circuit. ETT disconnections were separated by two 6-min duration baseline-ventilation intervals, over which heart rate, mean arterial/pulmonary artery pressure, cardiac output, and mixed-venous oxygen saturation values were recorded and averaged. Just prior to each ETT disconnection, mixed-venous and arterial blood gas samples were taken and analysed immediately (ABL System 625 blood-gas analyser model; Radiometer, Copenhagen, Denmark). After collecting the gases expired within 2 min prior to the second and third ETT disconnection, physiological dead space was determined as previously described [30]. Formula-derived variables included cardiac, systemic and pulmonary vascular resistance index, oxygen consumption/delivery, oxygen extraction ratio (O_2ER), right/left ventricular stroke work index (SWI), respiratory quotient, alveolar oxygen partial pressure (P_{O_2}), and shunt fraction (see Appendix 2).

ΔFRC and end-expiratory lung volume

Within 105–120 min after study-posture assumption, baseline-ventilation ΔFRC was determined twice as previously reported [32], by allowing exhalation to V_r. Expiratory V' always reached 0 $L \cdot s^{-1}$ within <10 s. The two ΔFRC measurements were separated by 17 min of baseline ventilation. Immediately after each ΔFRC measurement, FRC was determined with the closed-circuit helium dilution technique as previously explained [30, 33–35]. Helium concentration was measured with a helium-analyser (PK Morgan Ltd, Kent, UK). Helium-dilution technique limitations have been previously analysed [36]. Baseline ventilation EELV was computed as the sum of measured FRC and ΔFRC.

Statistical analysis

For each posture, only the means of obtained sets of measurements were analysed. Variable comparisons were conducted with two-factor univariate ANOVA for repeated measures, followed by the Scheffé test as appropriate. Significance was accepted at $p<0.05$. Values are presented as mean $\pm$ SD.

RESULTS

Full data were obtained from all study participants and no protocol-related complications occurred [37]. Of the 10 patients, six were weaned from mechanical ventilation 15.2 $\pm$ 3.1 days after its institution and discharged from the intensive care unit (ICU) after another 2–3 days and four patients died of multiple system organ failure (table 1).

ΔFRC, $PEEP_{tot}$ of the RS and chest wall, and P_{ga} were unaffected by body posture (table 2). P_{oes} at V_r did not differ significantly among study postures (table 2). The mean maximal amplitude and mean rise rate of P_{oes}-cardiac oscillations (fig. 1), were similar (table 2). Consequently, the initial, correct oesophageal balloon positioning relative to the heart was maintained throughout the study period, and P_{oes} measurements were as accurate as possible in all study postures [23]. The oesophageal balloon technique has been adopted in previous studies and is considered adequate in the prone position [30, 33, 35, 38].

Tracheal pressure, oesophageal pressure and transpulmonary pressure

P_{aw} was unaffected by body posture (fig. 2a). P_1/P_2 of averaged P_{oes} tracings were higher in prone *versus* SR_{BAS}/SR_{PP} at $V_T \geq 0.6$ L ($p<0.05$–0.01; fig. 2b). Maximal P_L ($P_{max,L}$) was lower in prone/SR_{PP} *versus* SR_{BAS} at $V_T \geq 0.6$–0.8 L ($p<0.05$–0.01). The P_1 value of P_L ($P_{1,L}$) was lower in prone/SR_{PP} *versus* SR_{BAS} at $V_T \geq 0.4$–0.6 L ($p<0.05$–0.01).

TABLE 2 Variables reflecting dynamic hyperinflation, and oesophageal and gastric pressures and their changes

	Pre-prone semirecumbent	Prone	Post-prone semirecumbent
ΔFRC L[#]	0.34±0.13	0.31±0.15	0.27±0.12
$PEEP_{tot,RS}$ cmH_2O[#]	11.3±1.5	10.4±1.7	10.1±1.5
$PEEP_{tot,cw}$ cmH_2O[#]	2.8±0.4	3.3±0.7	2.6±0.4
P_{oes} at V_r cmH_2O	12.6±3.1	8.6±3.6	12.4±3.0
P_{ga} at V_r cmH_2O	9.6±3.7	12.9±3.9	10.1±3.5
$\Delta P_{max,ga}$ at 0.6 L V_T cmH_2O[#]	3.7±1.1	4.2±1.3	3.9±1.1
$\Delta P_{max,ga}$ at 1.0 L V_T cmH_2O	5.6±1.9	6.0±2.4	5.9±2.0
$\Delta P_{2,ga}$ at 0.6 L V_T cmH_2O[#]	3.3±0.9	3.9±1.1	3.6±1.0
$\Delta P_{2,ga}$ at 1.0 L V_T cmH_2O	5.3±1.5	5.7±1.9	5.5±1.6
Mean maximal amplitude in P_{oes} cmH_2O[¶]	2.0±1.2	1.7±1.0	2.1±1.3
Mean rise rate in P_{oes} $cmH_2O \cdot s^{-1}$[¶]	12.5±5.2	11.4±4.7	12.8±5.3

Data are presented as mean±SD. ΔFRC: change in functional residual capacity; $PEEP_{tot}$: total positive end-expiratory pressure; RS: respiratory system; cw: chest wall; P_{oes}: oesophageal pressure; V_r: respiratory system relaxation volume; P_{ga}: gastric pressure; $\Delta P_{max,ga}$: difference between maximal P_{ga} and P_{ga} at V_r; V_T: tidal volume; $\Delta P_{2,ga}$: difference between plateau P_{ga} and P_{ga} at V_r. [#]: values correspond to baseline ventilation conditions; [¶]: for each study posture, reported values are mean±SD of determined values during all sets of test breaths (see also fig. 1).

$P_{2,L}$ was lower in prone/SRPP *versus* SRBAS at $V_T \geq 0.6$ L ($p<0.05$–0.01; fig. 2c). $P_{max,L}/P_{1,L}$ (individual patient data not shown), and $P_{2,L}$ exhibited similar response patterns to posture change in all patients. Figure 3 displays individual $P_{2,L}V_T$ relationships.

EELV and V_T/EELV

In prone and SRPP, baseline-ventilation EELV was significantly higher *versus* SRBAS (by 30.3±1.6% and 23.9±1.0%, respectively, $p<0.01$; table 3). Accordingly, the baseline-ventilation V_T (0.6 L)/EELV ratio, was lower in prone and SRPP *versus* SRBAS (0.41±0.04 and 0.42±0.04, respectively, *versus* 0.58±0.05, $p<0.01$). The sigh (1.0 L) V_T/EELV ratio was also lower in prone and SRPP *versus* SRBAS (0.68±0.06 and 0.71±0.06, respectively, *versus* 0.97±0.09, $p<0.01$). V_T/EELV exhibited similar response patterns to body posture in all patients.

Respiratory mechanics

Figure 4 displays the main results for the respiratory mechanics. Static chest wall elastance was higher in prone *versus* SRBAS/SRPP at $V_T \geq 0.6$ L ($p<0.05$–0.01). Additional lung resistance was lower in prone/SRPP *versus* SRBAS at all employed V_Ts ($p<0.01$). Static lung elastance ($E_{stat,L}$) was lower in prone/SRPP *versus* SRBAS at $V_T \geq 0.6$ L ($p<0.05$–0.01).

Haemodynamics and gas exchange

Table 4 displays the main results. Directly determined haemodynamic variables were not significantly affected by posture change. The O_2ER exhibited sequential significant decreases from SRBAS to SRPP. Left vetricular SWI became higher in SRPP *versus* SRBAS. All gas exchange variables (including $P_{a,O_2}/F_{I,O_2}$, carbon dioxide arterial tension, shunt fraction, and physiological dead space) were significantly improved in prone/SRPP *versus* SRBAS.

DISCUSSION

The present study has shown that in severe ARDS [8, 13, 14, 20], prone positioning under PEEP optimisation reduces ventilation-induced stress (reflected by P_L) and strain (reflected by V_T/EELV) relative to 60° SRBAS; these effects are maintained within 2 h following return to 60° SRPP. Although only 10 patients were studied, individual response patterns of P_L and V_T/EELV to posture change were similar. Favourable results occur with a baseline (0.6 L) to 1.0 L V_Ts (range 8.2–17.6 $mL \cdot kg^{-1}$ PBW for participants in the present study). The lowest of the aforementioned V_Ts are similar to the 8–9 $mL \cdot kg^{-1} V_T$s routinely used by physicians studying/treating patients with acute lung injury/ARDS [9, 39–42]. Other pronation benefits, also maintained in SRPP, included decreased $E_{stat,L}$ and additional lung resistance, improved arterial oxygenation, and reduced shunt fraction and P_{a,CO_2} and physiological dead space; these findings are consistent with previously published results [30, 37, 43–45].

In the present study, PEEP was optimised to 4.0±0.9 cmH_2O lower values relative to the pre-study PEEP. PEEP optimisation was aimed at: 1) maintaining pre-study arterial oxygenation in SRBAS; and 2) allowing for a V_T increase of 1.7±0.2 $mL \cdot kg^{-1}$ PBW during the study period, without concomitant end-inspiratory stress increase to potentially injurious levels exceeding 30 cmH_2O ($P_{2,L}$ in fig. 2c) [5, 46]. Posture change from near-supine to steep SRBAS may have facilitated the achievement of the aforementioned ventilation goals by partially relieving abdominal/cardiac compression of dependent/caudal lung regions [14].

Substantial lung mechanics/gas exchange benefits were obtained only after the pronation manoeuvre. The selection of the 0.6 L baseline V_T probably facilitated the intratidal alveolar recruitment [30, 47]; the optimised PEEP probably facilitated the maintenance of such recruitment [47]. Also, the employed 1.0 L sighs were probably more effective in the prone position [48]. The combined EELV and $P_{a,O_2}/F_{I,O_2}$ increases and the shunt fraction decrease indicate effective re-aeration of well perfused, but previously collapsed lung units [18, 23, 30, 49]. The $P_{2,L}$ and $E_{stat,L}$ reductions indicate pronation-induced reversal of regional atelectasis [23, 30].

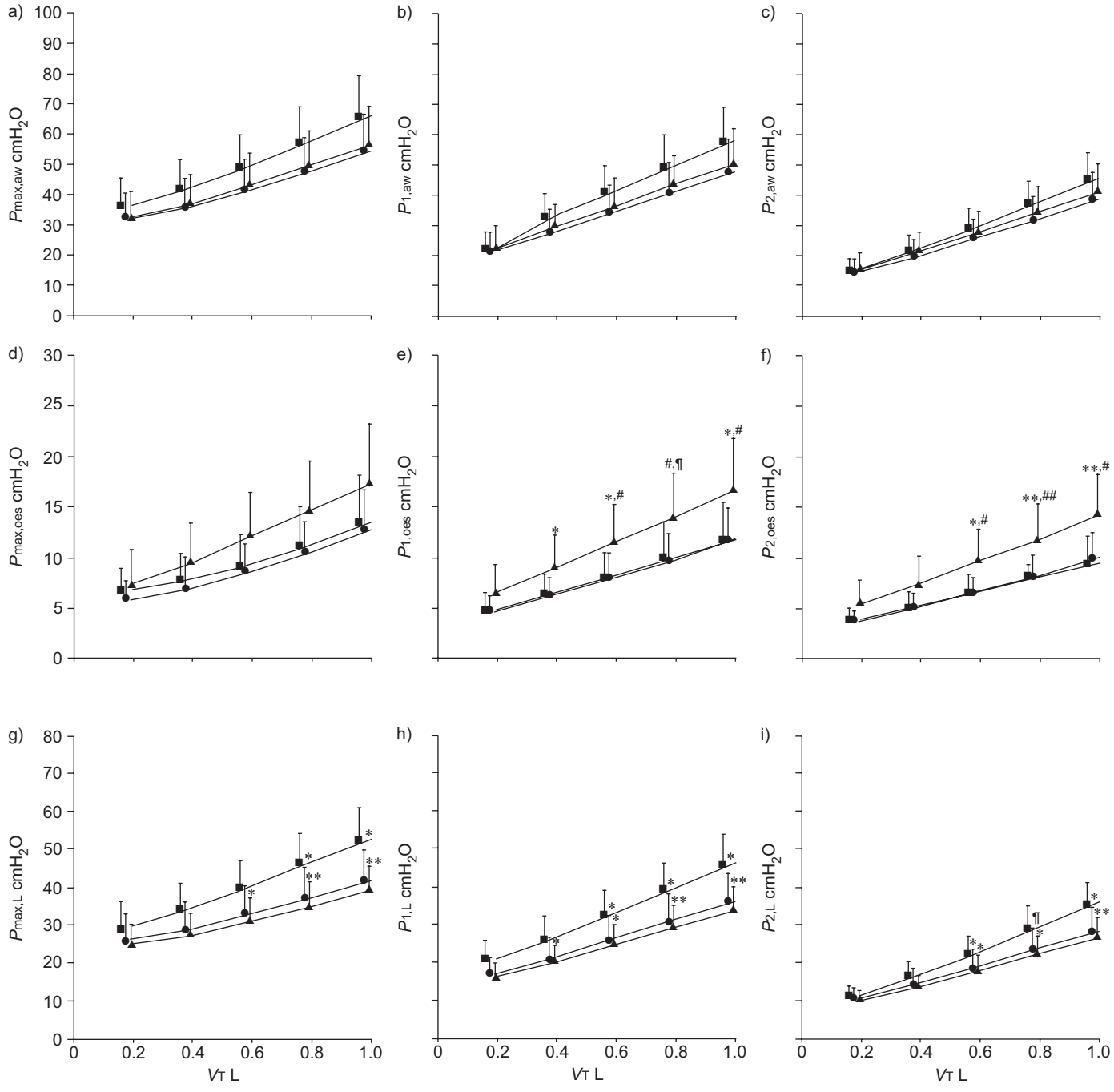

FIGURE 2. Results on tracheal (P_{aw}), oesophageal (P_{oes}) and transpulmonary (P_L) pressures from the iso-flow experiments. a–c) Average relationships of peak P_{aw} ($P_{max,aw}$), P_{aw} immediately after end-inspiratory airway occlusion ($P_{1,aw}$), and plateau P_{aw} ($P_{2,aw}$) with increasing inflation volume. d–f) Average relationships of peak P_{oes} ($P_{max,oes}$), P_{oes} immediately after end-inspiratory airway occlusion ($P_{1,oes}$), and plateau P_{oes} ($P_{2,oes}$) with inflation volume. g–i) Average relationships of peak P_L ($P_{max,L}$), P_L immediately after end-inspiratory airway occlusion ($P_{1,L}$), and plateau P_L ($P_{2,L}$) with inflation volume (V_T). Symbols represent mean values and bars represent SD. ■: pre-prone semirecumbent; ●: post-prone semirecumbent; ▲: prone. *: $p<0.05$ *versus* pre-prone semirecumbent (SR_{BAS}); **: $p<0.01$ *versus* SR_{BAS}; #: $p<0.05$ *versus* post-prone semirecumbent (SR_{PP}); ##: $p<0.01$ *versus* SR_{PP}; ¶: trend towards significance *versus* SR_{BAS}.

The P_{a,CO_2} and physiological dead space reductions suggest an increase in effective alveolar ventilation [23]. The additional lung resistance decrease suggests a reduced time constant inequality range, more homogenous lung inflation, and reduced numbers of atelectatic and hyperinflated/overdistended alveoli [14, 23, 30]. The reduction in regional atelectasis attenuates the stress in neighbouring lung regions [46]. The reduction in regional hyperinflation or overdistension attenuates regional strain and reduces the regional probability of traumatic alveolar rupture [23]. Thus, although the current authors could not directly determine regional stress/strain, the combined results in the present study

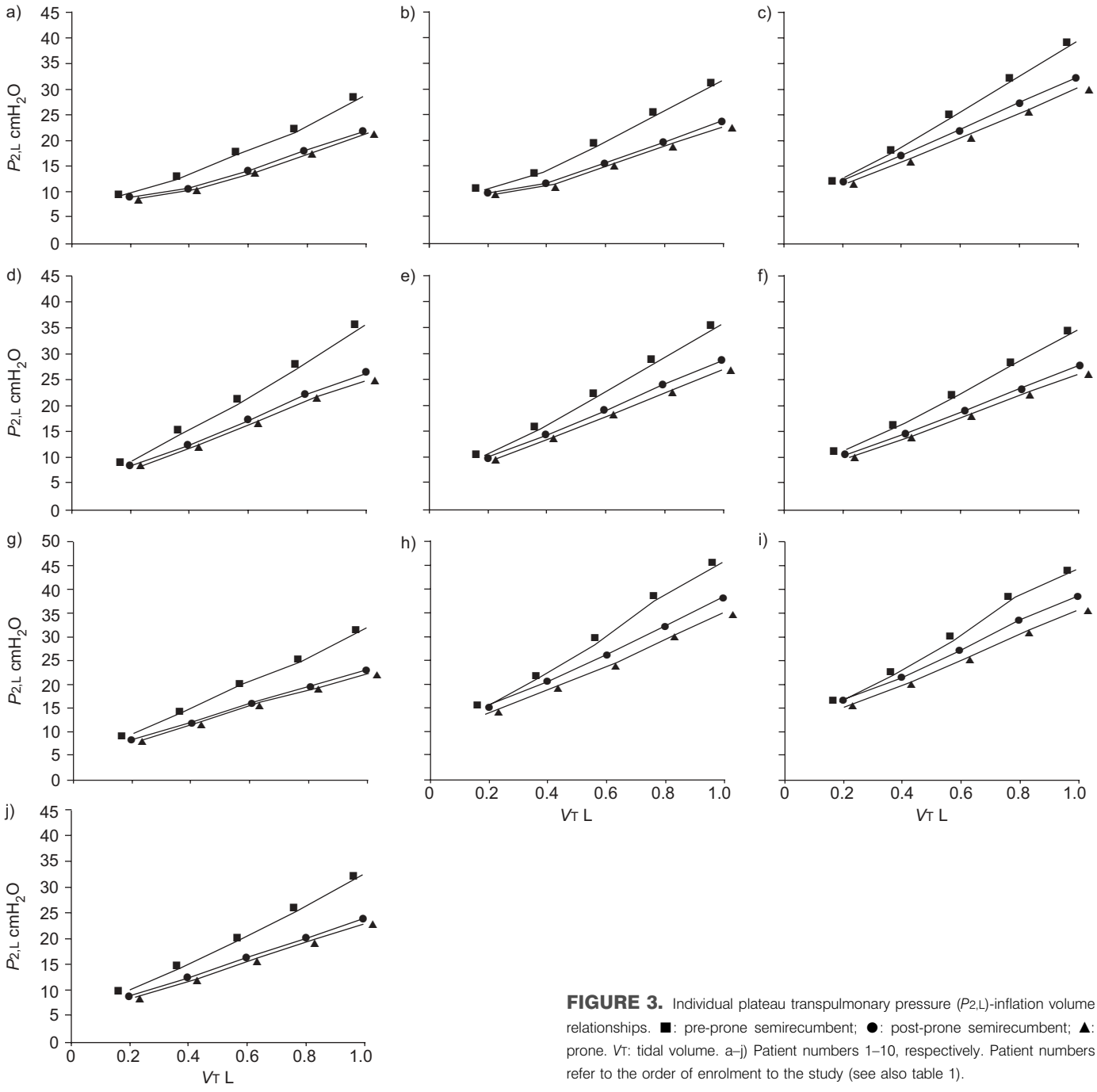

FIGURE 3. Individual plateau transpulmonary pressure ($P_{2,L}$)-inflation volume relationships. ■: pre-prone semirecumbent; ●: post-prone semirecumbent; ▲: prone. V_T: tidal volume. a–j) Patient numbers 1–10, respectively. Patient numbers refer to the order of enrolment to the study (see also table 1).

strongly suggest reduced ''regional probability'' of VILI in the prone position.

The observed significant decreases in O_2ER were due to the simultaneous decreases in oxygen consumption and/or increases in oxygen delivery. These changes could be attributable to the effects of the probably slowly increasing plasma propofol and fenanyl concentrations throughout the study period [50]. Propofol/fentanyl anaesthesia reduces oxygen consumption in hypoxaemic respiratory failure patients [24]. Mild and moderate maintenance infusion-induced increases in propofol and fentanyl plasma concentrations, respectively [50], should not directly affect myocardial performance [51, 52]. The observed arithmetical decreases in heart rate could be attributable to fentanyl [53]. The heart rate changes could have contributed to the observed arithmetical increases in SRPP cardiac index (table 4) by improving cardiac diastolic filling, cardiac muscle fibre length-tension relationship, and consequently, cardiac contractility [54]. The speculation for improved diastolic filling is supported by the observed

TABLE 3 End-expiratory lung volume (in L) during baseline ventilation

Patient No.	Pre-prone semirecumbent	Prone	Post-prone semirecumbent
1	1.17	1.64	1.60
2	1.09	1.57	1.50
3	0.96	1.35	1.31
4	1.05	1.54	1.45
5	0.99	1.39	1.34
6	1.02	1.51	1.42
7	1.11	1.59	1.53
8	0.89	1.33	1.26
9	0.92	1.30	1.28
10	1.14	1.61	1.58
Mean±SD	1.03±0.09	1.48±0.13**	1.43±0.12**

Data are presented as individual patient values. **: p<0.01 *versus* pre-prone semirecumbent.

increase in left ventricular SWI [55]. In SRPP, the improved haemodynamic performance could have contributed to the maintenance of the pronation gas exchange benefits relative to SRBAS. However, as in the case of the prone position, the major portion of the SRPP gas exchange improvement could still be explained by the still improved shunt fraction and physiological dead space (table 4), and thus, ventilation-perfusion matching.

The determinations of P_{oes} in different body postures may be problematic, despite prior relevant methodological interpretations [30, 33, 35, 38], and confirmation of an unchanged pattern of transmission of intracardiac pressure changes to the oesophageal balloon [23]. Pronation causes redistribution of regional lung collapse [56]; if this occurs in lung areas adjacent to the lower oesophagus, the patterns of intrapleural pressure transmission to the oesophageal balloon may differ between prone and semirecumbent postures, thus resulting in possible posture-related bias in P_L calculations. However, regional lung collapse, although different in amount, should tend to exhibit similar distribution in SRBAS and SRPP. This should have minimised the impact of the aforementioned potential problem upon the P_L results in the current study, because similar improvement in gas exchange, indicating similar amount of alveolar recruitment, was accompanied by similar reductions in P_L determined in prone and SRPP relative to SRBAS. Consequently, P_L was probably calculated in prone as accurately as in semirecumbent posture.

Pronation benefits were maintained during SRPP measurements; major contributory factors may include: 1) optimised PEEP-induced maintenance of overall pronation-induced alveolar recruitment, despite its posture-associated redistribution [56]; and 2) partial maintenance of a possible pronation-induced lower lung lobe decompression in steep semirecumbent posture [14]. The maintenance of lower lobe decompression could have been facilitated by the absence of abnormally raised intra-abdominal pressure and decreased abdominal compliance (table 2) [27].

Clinical implications

According to the lung stress/strain results presented in the current study, ventilation with standard V_Ts (0.6 L= 9.0±0.9 mL·kg^{-1} PBW) [9, 39–42] in prone/SRPP is equally protective as ventilation with low V_Ts (0.4 L=6.0±0.6 mL·kg^{-1} PBW) [25] in SRBAS. Indeed, in prone and SRPP, $P_{2,L}$ and $P_{max,L}$ values at baseline (0.6 L) V_T were similar to SRBAS$P_{2,L}$ and $P_{max,L}$ values at 0.4 L V_T (fig. 2c). V_T/EELV (strain) was also similar in prone and SRPP at 0.6 L V_T and SRBAS at 0.4 L V_T (0.39±0.04). Consequently, if in severe ARDS, low V_Ts are accepted as the ''gold standard'' in SRBAS [12, 25, 57], pronation may provide considerable ''V_T-liberation capability'' by allowing a 50% (3 mL·kg^{-1} PBW) V_T increase, without appreciable increase in the VILI risk. Under PEEP optimisation, such V_T liberation may be allowable in SRPP for at least 2 h.

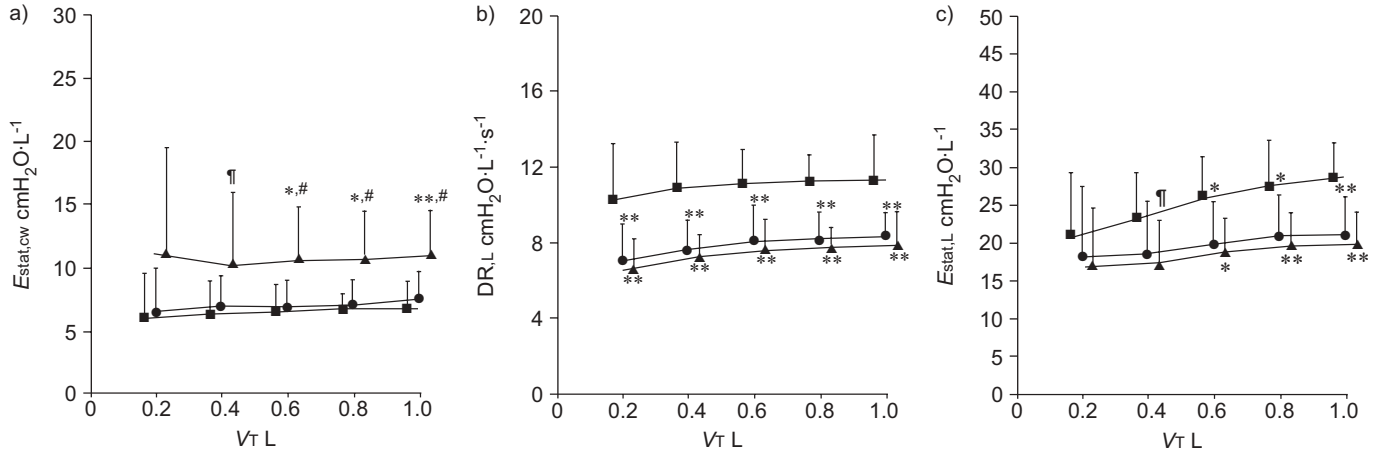

FIGURE 4. Partitioned respiratory mechanics. Data are presented as mean±SD. ■: pre-prone semirecumbent; ●: post-prone semirecumbent; ▲: prone. Symbols represent mean values and bars represent SD. E_{stat}: static elastance; cw: chest wall; DR: additional resistance; L: lung. *: p<0.05 *versus* pre-prone semi-recumbent; **: p<0.01 *versus* pre-prone semirecumbent; #: p<0.05 *versus* post-prone semirecumbent; ¶: trend towards significance *versus* pre-prone semirecumbent.

TABLE 4 Haemodynamic and gas exchange variables. Gas exchange results correspond to baseline ventilation.

	Body posture		
	BAS semirecumbent	Prone	Post-prone semirecumbent
Haemodynamic variables			
HR beats·min^{-1}	119±14	113±13	111±13
MAP mmHg	71±7	75±7	76±7
CVP mmHg	9±2	10±2	10±2
MPAP mmHg	27±4	28±4	28±4
PAWP mmHg	11±2	11±2	12±2
CI L·min^{-1}·m^{-2}	4.3±0.6	4.4±0.7	4.6±01.0
SVRI dynes·s·cm^{-5}·m^{-2}	1181±242	1218±278	1215±312
PVRI dynes·s·cm^{-5}·m^{-2}	293±50	302±56	300±68
V'_{O_2} mL·min^{-1}·m^{-2}	142±22	148±25	145±24
O_2ER	0.38±0.03	0.35±0.02$^{\#}$	0.32±0.02$^{\#,+}$
LVSWI g·m^{-1}	29.4±3.3	33.2±4.3	35.7±6.6¶
Gas exchange			
$P_{a,O_2}/F_{i,O_2}$ mmHg	86±7	133±13$^{\#}$	128±13$^{\#}$
P_{a,CO_2} mmHg	49.4±1.6	42.8±1.2$^{\#}$	43.9±1.2$^{\#}$
pHa	7.33±0.02	7.40±0.01$^{\#}$	7.39±0.01$^{\#}$
P_{v,O_2} mmHg	36.2±1.8	41.5±1.7$^{\#}$	43.2±2.1$^{\#}$
S_{v,O_2} %	57±2	66±2$^{\#}$	69±2$^{\#}$
P_{v,CO_2} mmHg	55.4±1.6	48.1±1.3$^{\#}$	49.4±1.3$^{\#}$
pHv	7.28±0.02	7.35±0.01$^{\#}$	7.34±0.01$^{\#}$
Qs·Qt^{-1}	0.36±0.03	0.24±0.03$^{\#}$	0.26±0.03$^{\#}$
V_d·V_t^{-1}	0.48±0.06	0.33±0.08$^{\#}$	0.35±0.07$^{\#}$

Data are presented as mean±SD. BAS: baseline; HR: heart rate; MAP: mean arterial pressure; CVP: central venous pressure; MPAP: mean pulmonary artery pressure; PAWP: pulmonary artery wedge pressure; CI: cardiac index; SVRI: systemic vascular resistance index; PVRI: pulmonary vascular resistance index; V'_{O_2}: oxygen consumption; O_2ER: oxygen extraction ratio; LVSWI: left ventricular stroke work index; P_{a,O_2}: arterial oxygen tension; F_{I,O_2}: inspired oxygen fraction; P_{a,CO_2}: carbon dioxide arterial tension; pHa: arterial pH; P_{v,O_2}: mixed venous oxygen partial pressure; S_{v,O_2}: mixed venous oxygen saturation; P_{v,CO_2}: mixed venous carbon dioxide partial pressure; pHv: mixed venous pH; Qs·Qt^{-1}: shunt fraction; V_d·V_t^{-1}: physiological dead space. $^{\#}$: p<0.01 *versus* SRBAS; ¶: p<0.05 *versus* pre-prone semirecumbent (SRBAS); $^{+}$: p<0.05 *versus* prone. 1 mmHg=0.133 kPa.

Sighs frequently improve oxygenation in ARDS [34, 48, 58]. The present authors administered 1.0-L sigh-test V_Ts (15.0±1.5 mL·kg^{-1} PBW), which resulted in significantly lower P_L (fig. 3) and V_T/EELV in prone/SRPP. These results indicate a decreased probability of traumatic alveolar rupture, especially during frequent sigh administration (1–3·min^{-1}) [34, 48].

Conclusions

Prone positioning of patients with early and severe acute respiratory distress syndrome reduces lung parenchyma stress and strain during mechanical ventilation. This suggests a reduced risk of ventilator-induced lung injury. Pronation also improves sigh safety and gas exchange efficiency. Under positive end-expiratory pressure optimisation, pronation benefits may be maintained in a post-prone semirecumbent position.

ACKNOWLEDGMENTS

The authors would like to thank M. Tzoufi for her valuable help in manuscript preparation.

APPENDIX 1: INSPIRATORY MECHANICAL VARIABLES

For the respiratory system, chest wall, and lung the following inspiratory mechanics-variables were determined: 1) maximal, interrupter, and additional resistances, computed respectively as P_{max}–P_2, P_{max}–P_1, and P_1–P_2 differences divided by the preceding inspiratory flow; and 2) dynamic, and static elastances, computed as respective P_1–$PEEP_{tot}$ and P_2–$PEEP_{tot}$ differences divided by the administered V_T. Lung interrupter resistance reflects ''ohmic'' airway resistance; lung additional resistance reflects lung tissue stress relaxation tension and time constant inequality.

APPENDIX 2: FORMULAS USED TO DERIVE HAEMODYNAMIC AND GAS EXCHANGE VARIABLES

Formulas used to derive haemodynamic and gas exchange variables [59, 60]

1. Cardiac index=CO/BSA
2. Systemic vascular resistance index=(MAP–CVP)×80×CI^{-1}
3. Pulmonary vascular resistance index=(MPAP–PAWP)×80×CI^{-1}
4. Oxygen consumption per m^2 BSA=CI×1.36×Hgb×(S_{aO_2}–S_{vO_2})
5. Oxygen delivery per m^2 BSA=CI×1.36×Hgb×S_{a,O_2}
6. Oxygen extraction ratio=(S_{a,O_2}–S_{v,O_2})×S_{a,O_2}^{-1}
7. SVI=CI×(heart rate)$^{-1}$[61]
8. Right ventricular stroke work index=(MPAP–CVP)×SVI×0.0136 [61]
9. Left ventricular stroke work index=(MAP–PAWP)×SVI×0.0136 [61]
10. Respiratory Quotient=(FEY of carbohydrate intake)×1.0+(FEY of protein intake)×0.8+(FEY of lipid intake)×0.7 [62]
11. Alveolar P_{O_2}=P_{i,O_2}–P_{A,CO_2}×[F_{I,O_2}–(1–F_{I,O_2})×R^{-1}]; P_{i,O_2}=F_{I,O_2}×(P_B–47); P_{A,CO_2}~P_{a,CO_2}
12. O_2 content of blood=Hgb×1.36×S_{O_2}×10–1+0.003×P_{O_2}
13. Shunt fraction=(C_{c,O_2}–C_{a,O_2})×(C_{c,O_2}–C_{v,O_2})–1

CO: cardiac output (L·min^{-1}); BSA: body surface area (m^2); MAP: mean arterial pressure (mmHg); CVP: central venous pressure (mmHg); 80: transformation factor of Wood units (mmHg·L^{-1}·min) to standard metric units (dynes·s·cm^{-5}); CI: cardiac index (L·min^{-1}·m^{-2}); MPAP: mean pulmonary artery pressure (mmHg); PAWP: pulmonary artery wedge pressure (mmHg); 1.36: O_2 combining power of 1 g of haemoglobin (mL); Hgb: haemoglobin concentration in g·L^{-1}; S_{a,O_2}: arterial O_2 saturation; S_{v,O_2}: mixed venous O_2 saturation; SVI: stroke volume index (mL per heart beat); 0.0136: conversion factor pressure and volume units to work units (g·m); FEY: fractional energy yield relative to total of prescribed nutritional support; P_{i,O_2}: inspired O_2 partial pressure (mmHg); P_{A,CO_2}: alveolar CO_2 partial pressure (mmHg); R: respiratory quotient; P_B: barometric pressure (mmHg); 47: water saturated vapour pressure at 37°C (mmHg); 0.003: O_2 solubility coefficient at 37°C (mL·dL^{-1}·mmHg); P_{O_2}: O_2 partial pressure (mmHg); S_{O_2}: oxygen

saturation; $C_{c,O_2}/C_{a,O_2}/C_{v,O_2}$: O_2 content in end-capillary/arterial/mixed-venous blood, respectively.

1 mmHg=0.133 kPa.

REFERENCES

1 Slutsky AS, Tremblay LN. Multiple organ system failure. Is mechanical ventilation a contributing factor? *Am J Respir Crit Care Med* 1998; 157: 1721–1725.
2 Slutsky AS. Lung injury caused by mechanical ventilation. *Chest* 1999; 116: Suppl. 1, S9–S15.
3 Gattinoni L, Carlesso E, Cadringher P, Valenza F, Vaginelli F, Chiumello D. Physical and biological triggers of ventilator-induced lung injury and its prevention. *Eur Respir J* 2003; 22: Suppl. 47, S15–S25.
4 Vlahakis NE, Schroeder MA, Limper AH, Hubmayr RD. Stretch induces cytokine release by alveolar epithelial cells *in vitro*. *Am J Physiol* 1999; 277: Suppl. 1, L167–L173.
5 Nahum A, Hoyt J, Schmitz L, Moody J, Shapiro R, Marini JJ. Effect of mechanical ventilation strategy on dissemination of intratracheally distilled *Escherichia coli* in dogs. *Crit Care Med* 1997; 25: 1733–1743.
6 Slutsky AS. The acute respiratory distress syndrome, mechanical ventilation, and the prone position. *N Engl J Med* 2003; 345: 610–611.
7 Pelosi P, Crotti S, Brazzi L, Gattinoni L. Computed tomography in adult respiratory distress syndrome: what has it taught us? *Eur Respir J* 1996; 9: 1055–1062.
8 Puybasset L, Cluzel P, Gusman P, *et al.* Regional distribution of gas and tissue in acute respiratory distress syndrome I. Consequences for lung morphology. *Intensive Care Med* 2000; 26: 857–869.
9 Eichacker PQ, Gerstenberger ER, Banks SM, Cui X, Natanson C. Meta-analysis of acute lung injury and acute respirtory distress syndrome trials testing low tidal volumes. *Am J Respir Crit Care Med* 2002; 166: 1510–1514.
10 Pinsky MR. The haemodynamic consequences of mechanical ventilation: an evolving story. *Intensive Care Med* 1997; 23: 493–503.
11 Albert RK, Kirk W, Pitts C, Butler J. Extra-alveolar vessel fluid filtration coefficients in excised and *in situ* canine lobes. *J Appl Physiol* 1985; 59: 1555–1559.
12 The National Heart, Lung, and Blood Institute ARDS Clinical Trials Network. Higher *versus* lower positive end-expiratory pressures in patients with the acute respiratory distress syndrome. *N Engl J Med* 2004; 351: 327–336.
13 Puybasset L, Gusman P, Muller JC, *et al.* Regional distribution of gas and tissue in acute respiratory distress syndrome III. Consequences for the effects of positive end-expiratory pressure. *Intensive Care Med* 2000; 26: 1215–1227.
14 Rouby JJ, Puybasset L, Nieszkowska A, Lu Q. Acute respiratory distress syndrome: lessons from computed tomography of the whole lung. *Crit Care Med* 2003; 31: Suppl. 4, S285–S295.
15 Vieira SR, Puybasset L, Lu Q, *et al.* A scanographic assessment of pulmonary morphology in acute lung injury: significance of the lower inflection point detected on the lung pressure-volume curve. *Am J Respir Crit Care Med* 1999; 159: 1612–1623.
16 Broccard AF, Shapiro RS, Schmitz LL, Adams AB, Nahum A, Marini JJ. Prone positioning attenuates and redistributes ventilator-induced lung injury in dogs. *Crit Care Med* 2000; 28: 295–303.
17 Nishimura M, Honda O, Tomiyama N, Johkoh T, Kagawa K, Nishida T. Body position does not influence the location of ventilator-induced lung injury. *Intensive Care Med* 2000; 26: 1664–1669.
18 Albert RK, Hubmayr RD. The prone position eliminates compression of the lungs by the heart. *Am J Respir Crit Care Med* 2000; 161: 1660–1665.
19 Gattinoni L, Pelosi P, Vitale G, Pesenti A, D' Andrea L, Mascheroni D. Body position changes redistribute lung computed-tomographic density in patients with acute respiratory failure. *Anesthesiology* 1991; 74: 15–23.
20 Rouby JJ, Puybasset L, Cluzel P, *et al.* Regional distribution of gas and tissue in acute respiratory distress syndrome II. Physiological correlations and definition of an ARDS Severity Score. *Intensive Care Med* 2000; 26: 1046–1056.
21 Bernard GR, Artigas A, Brigham KL, *et al.* The American-European consensus conference on ARDS. Definition, mechanisms, relevant outcomes, and clinical trial coordination. *Am J Respir Crit Care Med* 1994; 149: 818–824.
22 Pugh RN, Murray-Lyon IM, Dawson JL, Pietroni MC, Williams R. Transection of the esophagus for bleeding oesophageal varices. *Br J Surg* 1973; 60: 646–649.
23 Mentzelopoulos SD, Zakynthinos SG, Roussos C, Tzoufi MJ, Michalopoulos AS. Prone position improves lung mechanical behavior and enhances gas exchange efficiency in mechanically ventilated chronic obstructive pulmonary disease patients. *Anesth Analg* 2003; 96: 1756–1767.
24 Elsasser S, Schachinger H, Strobel W. Adjunctive drug treatment in severe hypoxic respiratory failure. *Drugs* 1999; 58: 429–446.
25 The Acute Respiratory Distress Syndrome Network. Ventilation with lower tidal volumes as compared with traditional tidal volumes for acute lung injury and the acute respiratory distress syndrome. *N Engl J Med* 2000; 342: 1301–1308.
26 Baydur A, Behrakis PK, Zin WA, Jaeger M, Milic-Emili J. A simple method for assessing the validity of the esophageal balloon technique. *Am Rev Respir Dis* 1982; 126: 788–791.
27 Ranieri VM, Brienza N, Santostasi S, *et al.* Impairment of lung and chest wall mechanics in patients with acute respiratory distress syndrome. Role of abdominal distention. *Am J Respir Crit Care Med* 1997; 156: 1082–1091.
28 Diehl JL, Lofaso F, Deleuze P, Similowski T, Lemaire F, Brochard L. Clinically relevant diaphragmatic dysfunction after cardiac operations. *Ann Thorac Surg* 1994; 107: 487–498.
29 Johnson B, Richard JC, Straus C, Mancebo J, Lemaire F, Brochard L. Presssure-volume curves and compliance in acute lung injury. Evidence of recruitment above the lower inflection point. *Am J Respir Crit Care Med* 1999; 159: 1172–1178.
30 Pelosi P, Tubiolo D, Mascheroni D, *et al.* Effects of the prone position on respiratory mechanics and gas exchange during acute lung injury. *Am J Respir Crit Care Med* 1998; 157: 387–393.
31 Tantucci C, Corbeil C, Chasse M, Braidy J, Matar N, Milic-Emili J. Flow resistance in patients with chronic obstructive

pulmonary disease in acute respiratory failure. *Am Rev Respir Dis* 1991; 144: 384–389.
32 Guérin C, Coussa ML, Eissa NT, *et al.* Lung and chest wall mechanics in mechanically ventilated COPD patients. *J Appl Physiol* 1993; 74: 1570–1580.
33 Pelosi P, Croci M, Callapi E, *et al.* Prone positioning improves pulmonary function in obese patients during general anesthesia. *Anesth Analg* 1996; 83: 578–583.
34 Patroniti N, Foti G, Cortinovis B, *et al.* Sigh improves gas exchange and lung volume in patients with acute respiratory distress syndrome undergoing pressure support ventilation. *Anesthesiology* 2002; 96: 788–794.
35 Pelosi P, Croci M, Calappi E, *et al.* The prone positioning during general anesthesia minimally affects respiratory mechanics while improving functional residual capacity and increasing oxygen tension. *Anesth Analg* 1995; 80: 955–960.
36 Pelosi P, Croci M, Ravagnan I, *et al.* Respiratory system mechanics in sedated, paralyzed, morbidly obese patients. *J Appl Physiol* 1997; 83: 811–818.
37 Gattinoni L, Tognoni G, Pesenti A, *et al.* Effect of prone positioning on the survival of patients with acute respiratory distress syndrome. *N Engl J Med* 2001; 345: 568–573.
38 Milic-Emili J, Mead J, Turner JM. Topography of esophageal presssure as a function of posture in man. *J Appl Physiol* 1964; 19: 212–216.
39 Thompson BT, Hayden D, Matthay MA, Brower R, Parsons PE. Clinicians' approaches to mechanical ventilation in acute lung injury and ARDS. *Chest* 2001; 120: 1622–1627.
40 Esteban A, Anzueto A, Alia I, *et al.* How is mechanical ventilation employed in the intensive care unit? An international utilization review. *Am J Respir Crit Care Med* 2000; 161: 1450–1458.
41 Carmichael LC, Dorinsky PM, Higgins SB, *et al.* Diagnosis and treatment of acute respiratory distress syndrome in adults: an international survey. *J Crit Care* 1996; 11: 9–18.
42 Esteban A, Anzueto A, Frutos F, *et al.* Characteristics and outcomes in adult patients receiving mechanical ventilation: a 28-day international study. *JAMA* 2002; 287: 345–355.
43 Friedrich P, Krafft P, Hochleuthner H, Mauritz W. The effects of long-term prone positioning in patients with trauma-induced adult respiratory distress syndrome. *Anesth Analg* 1996; 83: 1206–1211.
44 Pelosi P, Bottino N, Chiumello D, *et al.* Sigh in supine and prone position during acute respiratory distress syndrome. *Am J Respir Crit Care Med* 2003; 167: 521–527.
45 Gattinoni L, Vagginelli F, Carlesso E, *et al.* Decrease in $PaCO_2$ with prone position is predictive of improved outcome in acute respiratory distress syndrome. *Crit Care Med* 2003; 31: 2727–2733.
46 Mead J, Takishima T, Leith D. Stress distribution in lungs: a model of pulmonary elasticity. *J Appl Physiol* 1970; 28: 596–608.
47 Gattinoni L, Pelosi P, Crotti S, Valenza F. Effects of positive end-expiratory pressure on regional distribution of tidal volume and recruitment in adult respiratory distress syndrome. *Am J Respir Crit Care Med* 1995; 151: 1807–1814.
48 Pelosi P, Bottino N, Chiumello D, *et al.* Sigh in supine and prone position during acute respiratory distress syndrome. *Am J Respir Crit Care Med* 2003; 167: 521–527.
49 Mure M, Domino KB, Lindahl SGE, Hlastala MP, Altemeier WA, Glenny RB. Regional ventilation-perfusion distribution is more uniform in the prone position. *J Appl Physiol* 2000; 88: 1076–1083.
50 Glass PSA, Shafer SL, Reves JG. Intravenous drug delivery systems. *In*: Miller RD, ed. Anesthesia. 5th Edn. New York, Churchill Livingstone, 2000; pp. 377–412.
51 Quattara A, Langeron O, Souktani R, Mouren S, Coriat P, Riou B. Myocardial and coronary effects of propofol in rabbits with compensated cardiac hypertrophy. *Anesthesiology* 2001; 95: 699–707.
52 Kohno K, Takaki M, Ishioka K, *et al.* Effects of intracoronary fentanyl on left ventricular mechanoenergetics in the excised cross-circulated canine heart (revised publication). *Anesthesiology* 1997; 87: 658–666.
53 Lokker GJ, Mader RM, Rizovski B, *et al.* Negative chronotropic effects of fentanyl attenuate beneficial effects of dobutamine on oxygen metabolism: hemodynamic and pharmacokinetic interactions. *J Pharmacol Exp Ther* 1999; 290: 43–50.
54 Blanck TJJ, Lee DL. Cardiac Physiology. *In*: Miller RD, ed. Anesthesia. 5th Edn. New York, Churchill Livingstone, 2000; pp. 619–646.
55 Glower DD, Spratt JA, Snow ND, *et al.* Linearity of the Frank-Starling relationship in the intact heart: the concept of preload recruitable stroke work. *Circulation* 1985; 71: 994–1009.
56 Gattinoni L, Pelosi P, Vitale G, Pesenti A, D' Andrea L, Mascheroni D. Body position changes redistribute lung computed-tomographic density in patients with acute respiratory failure. *Anesthesiology* 1991; 74: 15–23.
57 Levy MM. PEEP in ARDS-how much is enough? *N Engl J Med* 2004; 351: 389–391.
58 Grasso S, Mascia L, Del Turco M, *et al.* Effects of recruiting maneuvers in patients with acute respiratory distress syndrome ventilated with protective ventilatory strategy. *Anesthesiology* 2002; 96: 795–802.
59 Mark JB, Slaughter TF, Reves JG. Cardiovascular monitoring. *In*: Miller RD, ed. Anaesthesia. 5th Edn. New York, Churchill Livingstone, 2000; pp. 1117–1230.
60 Moon ME, Camporesi EM. Respiratory monitoring. *In*: Miller RD, ed. Anaesthesia. 5th Edn. New York, Churchill Livingstone, 2000; pp. 1255–1296.
61 Marino PL. The pulmonary artery catheter. *In*: Marino PL, ed. The ICU book. 2nd Edn. Baltimore, Williams & Wilkins, 1997; pp. 154–165.
62 Marino PL. Nutrient and energy requirements. *In*: Marino PL, ed. The ICU book. 2nd Edn. Baltimore, Williams & Wilkins, 1997; pp. 721–736.